

Adaptive Wasserstein Hourglass for Weakly Supervised Hand Pose Estimation from Monocular RGB

Yumeng Zhang¹, Li Chen¹, Yufeng Liu², Junhai Yong¹, Wen Zheng²

¹School of Software, Tsinghua University, Beijing, China

²Y-tech, Kwai, Beijing, China

Abstract

Insufficient labeled training datasets is one of the bottlenecks of 3D hand pose estimation from monocular RGB images. Synthetic datasets have a large number of images with precise annotations, but the obvious difference with real-world datasets impacts the generalization. Little work has been done to bridge the gap between two domains over their wide difference. In this paper, we propose a domain adaptation method called Adaptive Wasserstein Hourglass (AW Hourglass) for weakly-supervised 3D hand pose estimation, which aims to distinguish the difference and explore the common characteristics (e.g. hand structure) of synthetic and real-world datasets. Learning the common characteristics helps the network focus on pose-related information. The similarity of the characteristics makes it easier to enforce domain-invariant constraints. During training, based on the relation between these common characteristics and 3D pose learned from fully-annotated synthetic datasets, it is beneficial for the network to restore the 3D pose of weakly labeled real-world datasets with the aid of 2D annotations and depth images. While in testing, the network predicts the 3D pose with the input of RGB.

Introduction

The broad prospects in the fields of VR/AR applications, gesture recognition and robot control make hand pose estimation always be a research focus in the computer vision. In recent years, monocular RGB image-based 3D hand pose estimation (Boukhayma, De Bem, and Torr 2019; Ge et al. 2019; Iqbal et al. 2018; Spurr et al. 2018; Zimmermann and Brox 2017) has made great progress by means of powerful deep learning methods. Nevertheless, this task remains particularly difficult. Firstly, hand pose is so diverse that there are lots of self-occlusion from single viewpoint. Secondly, 3D estimations from single RGB image is an ill-posed problem due to inherent scale and depth ambiguities. These problems make it difficult to annotate the training data, which is crucial for the performance of deep learning methods.

Making use of synthetic data (Boukhayma, De Bem, and Torr 2019; Ge et al. 2019; Cai et al. 2018; Mueller et al. 2018; Zimmermann and Brox 2017), which is of high sufficiency, is the mainstream method to make up the deficiency

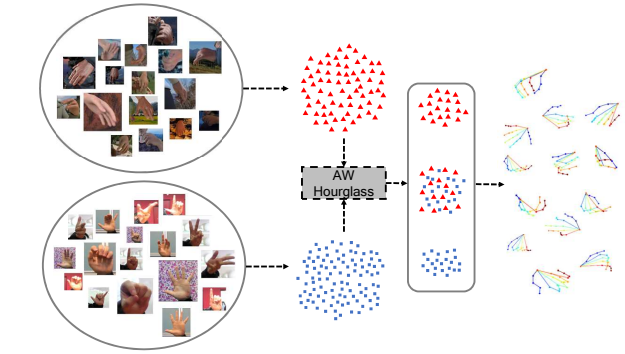


Figure 1: We propose the Adaptive Wasserstein Hourglass to improve the performance of weakly-labeled real-world datasets. Our method distinguishes common hand characteristics and dissimilar properties between synthetic and real-world datasets automatically and bridges the gap between common hand characteristics. As a result, The network begins to notice the common characteristics of hand between two domains, which are beneficial for generalization.

of training data in hand pose estimation. Zimmermann and Brox (Zimmermann and Brox 2017) adopted the joint training method of synthetic and real-world datasets, neglecting the difference between the two datasets, which limits the accuracy. Rad et al. (Rad, Oberweger, and Lepetit 2018b) proposed a feature mapping method, which targets at the pose estimation in depth images, to eliminate the gap at the feature level. It requires same pose in synthetic image and corresponding real-world image, which is difficult to apply to pose estimations from monocular RGB images. Mueller et al. (Mueller et al. 2018) tried to narrow the gap by adopting CycleGan (Zhu et al. 2017) to improve the validity of synthetic images without paired images, but the requirement of only hands images included in real world turns it to be labor intensive. Boukhayma et al. (Boukhayma, De Bem, and Torr 2019) made use of synthetic datasets to train an encoder to predict the hand and camera parameters so that the camera intrinsic parameters are not necessary in the testing phase. However, like all the above-mentioned methods, this method

rely on the 3D annotations of real-world datasets, which are more difficult to acquire than camera intrinsics parameters in real-world applications. In order to ease dependence on costly 3D annotations, Cai et al. (Cai et al. 2018) adopted 2.5D representation of hand to reduce the uncertainty of 3D pose and utilized synthetic data and the uncostly depth images as the constraints to restore it. Utilizing a large number of synthetic images for training, Ge et al. (Ge et al. 2019) proposed a graph network to simultaneously predict mesh and keypoint position, which works quite well so far without 3D annotations. Utilizing strong constraints to align the two domains is beyond consideration. This leaves room for improvement.

According to our observation, though synthetic and real-world images of hands differ in skin texture and backgrounds, the hand structure, bone length and bone ratio tend to be similar. In order to introduce stronger constraints, we make the network learn the common characteristics, which consist of essential pose-related information. As a result, the 3D predictions of real-world datasets would benefit from learning these characteristics. Domain adaptation methods (Ganin et al. 2016; Shen et al. 2018) are designed to learn the common feature but the big gaps between synthetic and real-world datasets and the high-nonlinear relations between pose and latent features make it difficult for the existing methods to enhance 3D predictions. Therefore, we propose the Adaptive Wasserstein Hourglass, which automatically distinguishes the common hand characteristics and dissimilar properties (e.g. background and texture) so as to bridge the gap of common hand characteristics between the two datasets. Our method finds commonalities between synthetic and real-world database with their differences considered so that the big gap between them can be solved flexibly.

We conduct several experiments to further improve the network, including the removal of intermediate supervision. In the experiments, we find that the introduction of intermediate supervision makes the features in the Adaptive Wasserstein Hourglass focus more on the annotated information, while neglecting some useful information for real-world 3D pose estimation. Thus the performance gets impacted in the end.

In a word, the main contributions of this paper are as follows:

- We propose an efficient metric to distinguish common hand characteristics and dissimilar properties between synthetic and real-world datasets.
- We propose the Adaptive Wasserstein Hourglass that explores the common characteristics of the synthetic and real-world hands, which can be used as a module in any existing methods with joint training of synthetic and real-world datasets.
- We study the influence of intermediate supervision in weakly-supervised scenario, which helps us to achieve a further improvement.

We conduct several experiments on two Benchmark datasets RHD (Zimmermann and Brox 2017) and STB (Zhang et al. 2017). As synthetic datasets are crucial for the accuracy of real-world datasets, it's unfair to compare the results with different synthetic datasets for training. Our

method raises the 3D pose estimation accuracy of real-world datasets by a large margin when compared with methods trained for the same datasets. The results of experiment are also competitive with the state-of-the-art (Ge et al. 2019) while only about one-tenth of the synthetic images are used. Mesh information is not be used for it requires complex structure to predict for neural networks.

Related Works

Hand Pose Estimation with Synthetic Datasets

With the development of the rendering technology, the validity of computer-generated pictures gets increasingly promoted. Some approaches (Cai et al. 2018; Mueller et al. 2018; Zimmermann and Brox 2017; Ge et al. 2019; Boukhayma, De Bem, and Torr 2019) utilized synthetic images to assist the real-world hand pose estimation. Franziska Mueller et al. (Mueller et al. 2017) proposed a SynthHands datasets and used it to train hand localization and keypoint regression network. Zimmermann et al. (Zimmermann and Brox 2017) proposed a rendered hand pose datasets to boost performance of real-world datasets. Boukhayma et al. (Boukhayma, De Bem, and Torr 2019) adopted the synthetic datasets to pretrain the encoder to predict the hand and camera parameters and Ge et al. (Ge et al. 2019) also proposed a synthetic datasets to train graph network. However, all these methods do not consider the domain gap between synthetic and real-world datasets. Mueller et al. (Mueller et al. 2018) proposed a CycleGan framework to make the synthetic datasets more realistic, but the obvious difference is still in existence. Mahdi et al. (Rad, Oberweger, and Lepetit 2018a) eliminate the gap between synthetic and real depth images and made the features of RGB images the same as depth images. However, their method takes the depth image for inference and the performance is greatly impacted when using synthetic depth images. Up to now, how to eliminate the domain differences between synthetic datasets and real datasets remains to be a challenge.

Domain Adaptation

Domain adaptation techniques (Ganin et al. 2016; Tzeng et al. 2017) aim at learning a domain invariant feature for further domain generalization. Domain adaptation methods are rarely applied to hand pose estimation. However, the task bears several resemblances to classification, image segmentation and human pose estimation. Thus, these methods can serve as meaningful reference for designing domain adaptation methods in hand pose estimation. Li et al. (Li et al. 2018) proposed a MMD-AAE framework to align the features extracted from multi-domains. Sankaranarayanan et al. (Sankaranarayanan et al. 2018) adopted an adversarial training framework for weakly segmentation. However, the relation between images' RGB values and 3D pose are far more nonlinear, so it requires stronger constraints to eliminate the domain gap. Many works in human pose estimation aim to eliminate the gap between datasets collected in laboratory environments and in the wild. Since specified human bone's length should be relatively stable, Zhou et al. (Zhou et al. 2017) proposed a GeoLoss to minimize the variance of bone

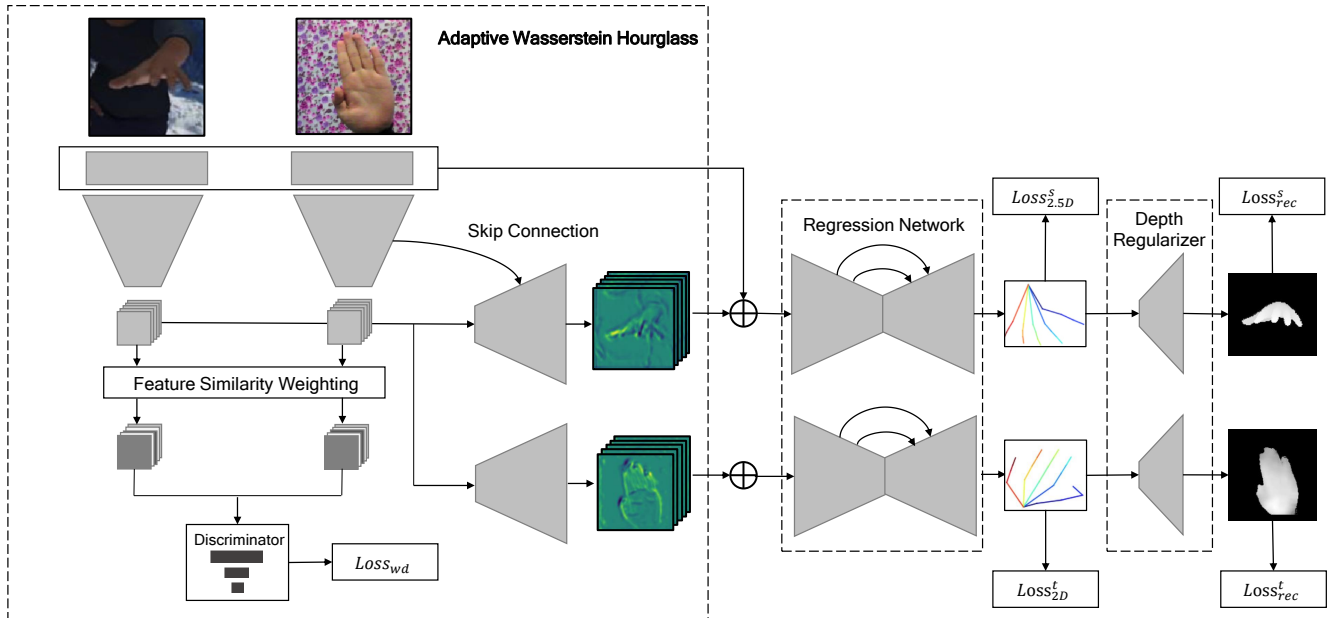


Figure 2: The overview of our network architecture. The Adaptive Wasserstein Hourglass uses the Feature Similarity Weighting to help network distinguish commonalities of hand and different features such as background. The discriminator is used to bridging the gap between weighted features, which helps network to explore the common characteristics of hand. We add depth regularizer to reduce the depth ambiguities of unlabeled real-world datasets. The subnetworks in the same dashed square mean that they share weights with each other.

length in a mini-batch as a weak supervision to align two datasets. However, the relation of the two datasets is not established. In contrast, a multi-domain classifier proposed by Yang et al. (Yang et al. 2018) views the visual information and relative offsets of the pose as domain prior knowledge to enhance the generalization ability. Although these methods make great achievements in human pose estimation, they are not suitable for hand pose estimation. It is the lacking of realism in synthetic hand rather than difference in background that greatly affects the generalization ability of the model. And some weak constraints failed for the diversity and serious self-occlusion of hand pose.

Methods

An overview of our method can be seen in Figure 2. Given a cropped RGB image of a hand $x \in \mathbb{R}^k$, we aim to get 3D pose of the hand, which is represented by the 3D positions of $K=21$ keypoints in camera coordinate system. In weakly supervised scenario, the study of the relation between latent features and 3D pose almost relies on the synthetic datasets in that only the synthetic datasets have both 2D and 3D annotations. At present, most of methods adopted joint training of two datasets directly and achieved good performance. However, undifferentiated joint training makes the network relies on large capacity to remember the features of the two domains, while ignoring the common hand characteristics of them, which reduces the advantageous effects of synthetic datasets on real-world datasets. In addition, dif-

ferences of two datasets such as backgrounds and skin texture are domain-specific, which should remain different in the latent space, while the commonalities of hands should be similar as these features are domain-invariant. Therefore, we propose the Adaptive Wasserstein Hourglass to learn the common characteristics by pulling closer features in the latent space selectively. As a result, the knowledge learned from the synthetic datasets can easily transfer to real-world datasets.

The proposed network architecture consists of three parts: Adaptive Wasserstein Hourglass, regression network and depth regularizer. Adaptive Wasserstein Hourglass extracts the fused features with attention of the common characteristics of two domains and then send the features to the regression network to get the 2.5D coordinates of K keypoints. The depth regularizer is also added to alleviate the depth ambiguities problems. In addition, the regression network and depth regularizer can be replaced by any type of network designed for weakly 3D pose estimation. In this paper, we adopt one of the most advanced network in existing methods.

Adaptive Wasserstein Hourglass

Extracting the features which consist of the common characteristics of two datasets facilitates the 3D pose estimation. However, the Figure 6a shows that there are obvious difference between the features extracted by the conventional model (Iqbal et al. 2018) with depth regularizer (Cai et al. 2018), from which we conclude that their network has not

the ability to recognize the common characteristics of two domains. Therefore, we design the Adaptive Wasserstein Hourglass to make up for this defect.

Wasserstein Metric The wasserstein distance is used to indicate the gap between features of source domain X_s and target domain X_t , where the source and target domain represent the synthetic and real-world datasets in our case. Given two continuous distributions p_r and p_θ , with joined distributions $\gamma(p_r, p_\theta)$, the wasserstein distance can be written as

$$W(p_r, p_\theta) = \inf_{\zeta \in \gamma} \int \int_{x,y} \|x - y\| \zeta(x, y) dx dy \quad (1)$$

$$= \inf_{\zeta \in \gamma} \mathbb{E}_{x,y} \zeta(\|x - y\|)$$

This original definition of wasserstein distance (1) is highly intractable (Arjovsky, Chintala, and Bottou 2017), while the Kantorovich-Rubinstein duality (Villani and dric 2009) demonstrates the distance can be reduced to (2) under certain conditions, which makes it possible for the neural networks to estimate this distance.

$$W(p_r, p_\theta) = \sup_{\|f\|_L \leq 1} \mathbb{E}_{s \sim p_r} [f(s)] - \mathbb{E}_{s \sim p_\theta} [f(t)] \quad (2)$$

where f is a function with Lipschitz constant of 1.

Wasserstein distance can be used for transfer learning (Shen et al. 2018). Given a feature representation z by a feature extractor $f_e : \mathbb{R}^k \rightarrow \mathbb{R}^n$. The goal of using wasserstein distance is to make the posterior probability $q_{\theta_e}(z|x_s)$ and $q_{\theta_e}(z|x_t)$ as similar as possible. A discriminator $f_d : \mathbb{R}^n \rightarrow \mathbb{R}$ is adopted to estimate the wasserstein distance by maximizing the following loss function:

$$\mathcal{L}_{wd}^*(x^s, x^t) = \mathbb{E}_{x^s \in X^s} [f_d(f_e(x^s))] - \mathbb{E}_{x^t \in X^t} [f_d(f_e(x^t))] \quad (3)$$

One approach to enforce the Lipschitz constraint is clipping the weights to $[-c, c]$ of the discriminator (Arjovsky, Chintala, and Bottou 2017). However, the gradient vanishing or exploding problems may be caused by this simply clipping. Thus Gulrajani et al. (Gulrajani et al. 2017) apply the gradient penalty to promote the convergence of network. The loss function can be written as

$$\mathcal{L}_g(x^s, x^t) = \mathcal{L}_{wd}(x^s, x^t) + \lambda_{gp} \mathbb{E}_{x_m \in X^m} (\|\nabla_{x_m} f(x_m)\|_2 - 1)^2 \quad (4)$$

where x^m is sampled from x^s and x^t with rate t , which uniformly sampled between 0 and 1.

Feature Similarity Metric There are differences in background and texture between synthetic datasets and real-world datasets, and the background and texture play an important role in determining the area of the hand. The existing domain adaptation methods ignore these differences directly, which results in the confusion of the network and increases the difficulty of the training. In order to solve this problem, we propose an adaptive feature similarity metric to distinguish different features.

Our Adaptive Wasserstein Hourglass takes a batch images of two domains (half-half) as input. Then these images are embedded into a latent space z by an encoder $E = f_e : \mathbb{R}^k \rightarrow \mathbb{R}^{C \times H \times W}$, where C represents the number of channels and (H, W) are the size of the features of per channel. The i_{th} channel of features of synthetic datasets are denoted as z_s^i , and those of real world datasets are denoted as z_t^i . We assume that the features of each channel represent a specific meaning because they are obtained through the same filter. At the same time, features of common hand characteristics should have similar patterns. Thus we define the following metric 5 to calculate the similarity between two datasets channel by channel.

$$\alpha^i(z_s, z_t) = \sum_{H \times W} \hat{z}_s^i \odot \hat{z}_t^i \quad (5)$$

\hat{z}^i means that the i_{th} channel of features is normalized.

We multiply \hat{z}_s^i and \hat{z}_t^i channel by channel after normalization, and then sum them up as the weight of the i_{th} channel of features. The more similar of the features, the higher weights are assigned. Thus in the process of pulling the weighted features of two domains closer to each other, features of common hand characteristics are drawn closer and closer, while features such as different background and texture remain the same.

The Wasserstein distance loss with feature similarity metric is shown in formula 6:

$$\mathcal{L}_{wd}(x^s, x^t) = \mathbb{E}_{x^s \in X^s} [f_d(\alpha(x_s, x_t) \times f_e(x^s))] - \mathbb{E}_{x^t \in X^t} [f_d(\alpha(x_s, x_t) \times f_e(x^t))] \quad (6)$$

Latent space z learning process adjusts the weights of encoder by back propagation and the decoder utilizes this unified latent space z to find proper representations for regression. As a result, the output of Adaptive Wasserstein Hourglass can be modified. We also add skipping connections to consolidate features across scales (Newell, Yang, and Deng 2016). The detail of the network architecture can be found in supplementary document.

Regression Module and Depth Regularizer

Scale Invariant 2.5D Representation: In order to alleviate the problem of depth ambiguities, we adopt the scale invariant 2.5D representation $P^{2.5D} = \{P_i^{2.5D}\}_{i=1}^K$, already used in (Sun et al. 2017; Cai et al. 2018; Iqbal et al. 2018), which consists of keypoint 2D locations in pixel coordinates

$P_i^{2D} = (x_i^p, y_i^p)$ and normalized root-relative depth value Z_i^n , which is obtained by subtracting the root coordinates and then normalized by making a specific bone length to a constant C.

$$P_i^n = \frac{C}{d} \cdot (P_i - P_{root}) \quad (7)$$

where P_{root} stands for the root coordinates and $d = \|P_{k1} - P_{k2}\|_2$ represents the length of chosen bone between $k1$ and $k2$ joints. We follow the same setting in (Cai et al. 2018), using the palm keypoint as the root keypoint. As for selecting the specific bone, we find that the 2D predictions of metacarpals are more stable leading us to choose these bones to normalize the coordinates.

Regression Network: (Iqbal et al. 2018) proposed a latent 2.5D heatmap network which achieves best accuracy in fully-supervised method. We adopt similar architecture for 2.5D pose estimation. We employ the L1 loss between predicted 2.5D coordinates $P^{2.5D}$ and the corresponding ground truth $(P^{2.5D})^{gt}$ to avoid using the designed target heatmaps, which is proved to be effective in (Iqbal et al. 2018). The regression loss is

$$\mathcal{L}_{2.5D}(P^{2.5D}, (P^{2.5D})^{gt}) = \sum_{i=1}^K (\|P_i^{2D} - (P_i^{2D})^{gt}\|_1 + \lambda_{alpha} \|Z_i^n - (Z_i^n)^{gt}\|_1) \quad (8)$$

where the K represents the number of keypoints.

Depth Regularizer: Depth images offer shape and depth information of the hand, which are good supplements in weakly-supervised scenario. We also adopt depth regularizer module similar to Cai et al. (Cai et al. 2018) to limit the range of depth prediction. The network takes 2D ground truth of keypoints and root-relative scale-normalized depth predictions as input and generates the normalized depth image D_n .

$$D_n = \sum_{i,j} \frac{d_{max} - d_{ij}}{d_{range}} \quad (9)$$

where the d_{max} and d_{range} represent the max depth value and depth range of hand, and d_{ij} represents the depth value at the location (i,j) .

The loss in this module can be written as follows:

$$\mathcal{L}_{reg}(D_n, D_{gt}) = \|D_n - D_{gt}\|_1 \quad (10)$$

Training

Combining the losses in Eq. (3), (8), (10), the overall loss can be obtained as

$$\mathcal{L} = -\lambda_{wd}\mathcal{L}_{wd} + \lambda_{res}(\mathcal{L}_{2.5D}^s + \mathcal{L}_{2d}^t) + \lambda_{reg}(\mathcal{L}_{reg}^s + \mathcal{L}_{reg}^t) \quad (11)$$

As the real-world datasets tend to have smaller number of images than synthetic datasets, we replicate some images of real-world datasets to make them equal. In the experiments, we find that pretrain the network on synthetic datasets without discriminator is crucial to achieve a high-quality pose estimation network. After pretraining, the whole network is trained in an end-to-end manner.

Experiments

Datasets and Metrics

Our model is trained with two publicly available datasets: Rendered Hand Pose Dataset (RHD) (Zimmermann and Brox 2017) and Stereo Hand Pose Tracking Benchmark (STB) (Zhang et al. 2017).

RHD is a synthetic hand pose datasets. It contains 41258 training images and 2728 test images. The training set contains 16 characters performing 31 actions and the test set has 4 characters performing 8 actions. Precise 2D and 3D annotations for 21 keypoints are provided, so are the mask of hands and depth images. There are large variations in view-points and hand poses, which can be a good learning reference for real-world datasets.

STB is a real-world datasets. It contains 12 sequences with 6 difference backgrounds. Stereo and depth images were captured from a Point Grey Bumblebee2 stereo camera and an Intel Real Sense F200 activate depth camera simultaneously. 2D and 3D annotations for 21 keypoints are provided.

End-Point-Error (EPE) and the Area Under the Curve (AUC) on percentage of correct keypoints are used to evaluate the performance of our method. We only report the performance of STB datasets since the synthetic datasets can be viewed as a constraint to restore the 3D pose of STB datasets in weakly supervised scenario. The coordinates relative to the root joint are sufficient in most of applications, thus we assume the global hand scale and the root depth are known in order to report EPE and PCK curve based on 3D hand joint locations in camera coordinate system, following the same condition used in (Zimmermann and Brox 2017; Cai et al. 2018).

Quantitative Results

Rethinking of the Intermediate Supervision: As there are no 3D annotations of real-world datasets, we think the intermediate supervision would lead the network to focus more on labeled information, neglecting the knowledge necessary for unlabeled 3D pose. To verify our idea, we conduct several experiments to study the influence of intermediate supervision using two-stack network of (Iqbal et al. 2018) with depth regularizer module (Cai et al. 2018) and the designed network in Figure 3, which adds some convolutional layers before 2.5D heatmaps and sends features in these layers instead of latent 2.5D heatmaps to the next stack.

The supervision at the first stack of (Iqbal et al. 2018) is denoted as FSS (First Stack Supervision) while supervision at the first stack of the designed network is denoted as FSSC (First Stack Supervision at additional Convolutional layer). To evaluate the performance of our method on Stereo

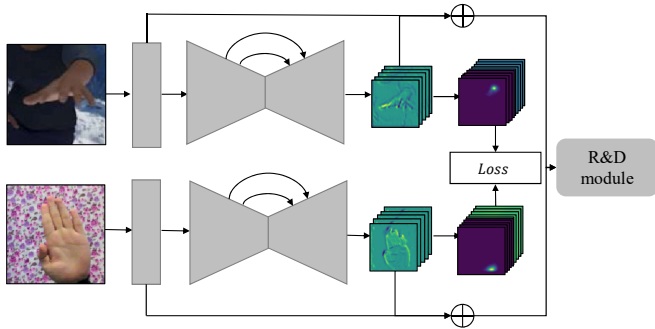


Figure 3: We add several convolution layers before the 2.5D heatmaps and send these features to the R&D module (Regression Network and Depth Regularizer). The goal of designing this network is to study the influence of intermediate loss on the heatmaps.

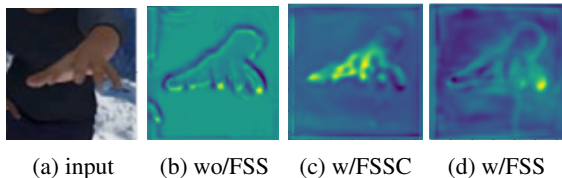


Figure 4: intermediate heatmaps

datasets, we follow the same evaluation protocol used in (Cai et al. 2018). We train the model with 10 sequences and test on the other 2 sequences.

As the experimental results shown in the Figure 5a, it can be observed that adding first stack supervision affects the accuracy greatly. In order to explore the reasons for the variations in accuracy, we visualize the first-stack heatmaps of w/FSS, w/FSSC and wo/FSS, as shown in Figure 4. The heatmaps of wo/FSS include rich information of the image while the other two mainly focus on a local region. Recently some meta learning methods (Bauer et al. 2017; Oreshkin, López, and Lacoste 2018) pointed out that a good feature extractor are crucial for generalization. Weakly supervised hand pose estimation can also be viewed as a generalization from synthetic datasets to real world datasets. Adding intermediate supervision makes the features so discriminative that some important information get lost, which impacts the performance.

In addition, we conduct experiments to study the influence of different losses in intermediate supervision. We denote 2D and 3D supervision of RHD (Zimmermann and Brox 2017) as R_{2D} and R_{3D} , while the 2D supervision of STB (Zhang et al. 2017) are denoted as S_{2D} . We add different losses in the first stack of (Iqbal et al. 2018) according to permutation and combination and the results are shown in Table 1.

From these experimental results, we conclude that the synthetic datasets annotations in the first stack affect the final performance of keypoint detection.

Experiments	3D Mean EPE(mm)	AUC@30mm
R2D	15.7	0.512
R3D	16.6	0.477
S2D	14.1	0.553
R2D+S2D	17.1	0.482
R2D+R3D	15.9	0.499
S2D+R3D	16.2	0.486
R2D+S2D+R3D	15.9	0.504
wo/IL	13.1	0.576

Table 1: The left column represents the losses added as intermediate supervision. wo/IL means that we don't use intermediate supervision.

Experiments	3D Mean EPE(mm)	AUC@30mm
wo/AWH+wo/FSS	13.1	0.576
w/WH+wo/FSS	13.1	0.578
w/AWH+wo/FSS	12.8	0.589

Table 2: Comparisons of 3D PCK results of five baselines with the proposed method

Baseline: To demonstrate the effectiveness of our Adaptive Wasserstein Hourglass, we compare the results with two baselines. For easier representation, the Adaptive Wasserstein Hourglass is denoted as AWH. Then the proposed method can be represented as w/AWH+wo/FSS. Together with the previous experiments, the two baselines are: a) wo/AWH+w/FSS: two-stack network in (Iqbal et al. 2018) with depth regularizer module. b) w/WH+wo/FSS: adding a domain adaptation module proposed by (Shen et al. 2018).

The results of these experiments are shown in Table 2. Although domain adaptation methods achieve good performance in classification, they are not suitable for 3D hand pose estimation, where two domains are quite different. We also test methods of (Tzeng et al. 2017; Ganin et al. 2016), but the network becomes extremely difficult to train. Based on above observations, we argue that there are some differences between two domains that can not be ignored. Thus we should distinguish the features, narrow the gap between the features of common hand characteristics while retaining difference of the features related to the background. This is the goal of our Adaptive Wasserstein Hourglass.

Comparisons with State-of-the-arts:

We compare our method with state-of-the-art fully-supervised and weakly-supervised methods. The comparisons are shown in Figure 5b. The methods with * represents the weakly supervised method which adopted same synthetic datasets as us. We achieve competitive results with some fully-supervised methods. Although the performance is slightly lower than Ge's (Ge et al. 2019) method, we only use a tenth number of synthetic images without mesh annotations and our approach is more expansive, which can be served as module to be added to existing methods.

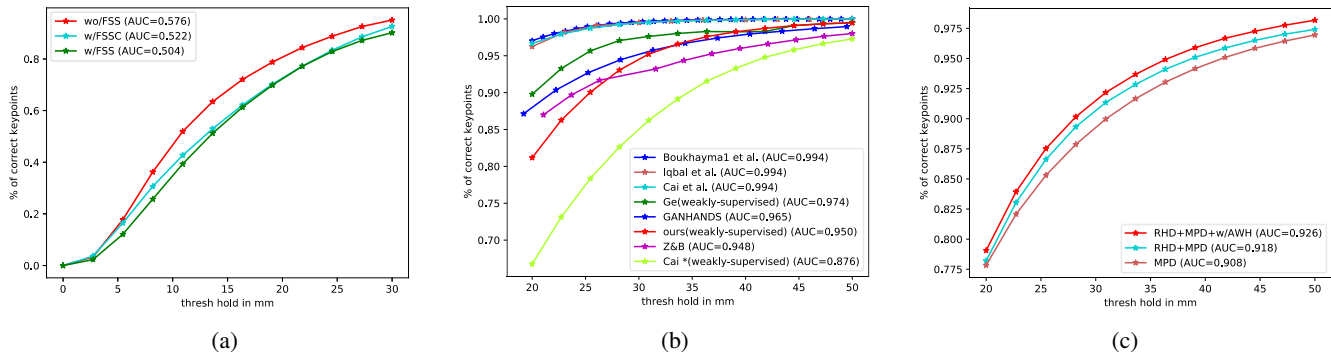


Figure 5: (a) Comparisons with designed baselines to study effects of intermediate supervision. (b) Comparisons with state-of-the-art methods. Our method outperforms some fully-supervised methods. (c) Experimental results on MPD (Gomezdonoso, Ortsescolano, and Cazorla 2019) datasets.

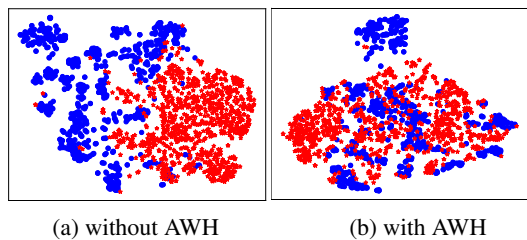


Figure 6: We randomly select 2000 samples of synthetic images and real-world images(half-half) and visualize their features by t-SNE (Maaten and Hinton 2008). The red points represent samples in source domain while the blue points represent samples the target domain.

Qualitative results

Several visual results of the proposed method are shown in Figure 7. We compare the results with Cai et al. (Cai et al. 2018), which adopted same training datasets and achieved second best results in existing weakly supervised methods. It can be seen that our model restores these hand pose with self occlusion correctly. More visual results can be found in supplementary document.

Feature Visualization: In order to investigate effectiveness of the latent features learned by our Wasserstein Hourglass, we use t-SNE (Maaten and Hinton 2008) to visualize these features extracted by two models—w/AWH+wo/FSS and wo/AWH+wo/FSS. A comparison between Figure 6a and Figure 6b reveals that Adaptive Wasserstein Hourglass has the ability to minimize the domain gap between similar features as well as keep the distance of domain-specific features.

Fully Supervised Scenario

Although our method is designed for weakly supervised scenario, we find it is still effective in fully supervised situation. We use the MPD (Gomezdonoso, Ortsescolano, and Cazorla 2019) real-world dataset, which have 82176 annotated samples, to test our method. Three experiments are done:

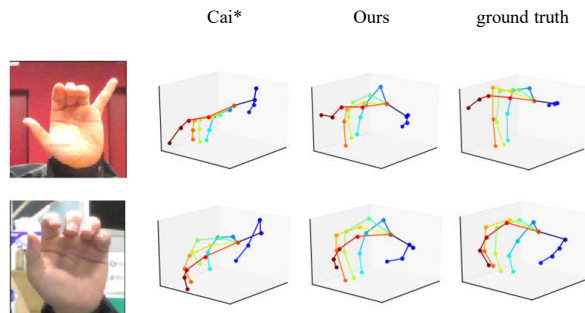


Figure 7: We compare our results with Cai et al (Cai et al. 2018). Our method predicts 3D pose more accurately and it even correctly restores the 3D pose with severe self occlusion.

a) solely training on MPD datasets(MPD). b)joint training with RHD (MPD+RHD). c) joint training with AWH module (RHD+MPD+w/AWH). The results are shown in Figure 5c. The PCK value has increased form 91.78% to 92.60% after adding the AWH module, which means that learning the common characteristics of hand helps improve the utilization of synthetic datasets.

Conclusion

We present a domain adaptation method for 3D hand pose estimation. We use the idea of meta learning for reference, and propose an adaptive feature extractor, which can extract common characteristics of hands in different domains while maintaining domain-specific features. Our method can effectively improve the accuracy, so as to be used as a module in other methods with good expansibility. In the future, we will try to combine the realization of synthetic datasets with domain adaptation methods to improve the utilization of synthetic datasets.

References

- Arjovsky, M.; Chintala, S.; and Bottou, L. 2017. Wasserstein generative adversarial networks. In *Proceedings of the 34th International Conference on Machine Learning, ICML 2017, Sydney, NSW, Australia, 6-11 August 2017*, 214–223.
- Bauer, M.; Rojas-Carulla, M.; Świątkowski, J. B.; Schölkopf, B.; and Turner, R. E. 2017. Discriminative k-shot learning using probabilistic models. *arXiv preprint arXiv:1706.00326*.
- Boukhayma, A.; De Bem, R.; and Torr, P. H. S. 2019. 3d hand shape and pose from images in the wild.
- Cai, Y.; Ge, L.; Cai, J.; and Yuan, J. 2018. Weakly-supervised 3d hand pose estimation from monocular rgb images. In *The European Conference on Computer Vision (ECCV)*.
- Ganin, Y.; Ustinova, E.; Ajakan, H.; Germain, P.; Larochelle, H.; Laviolette, F.; Marchand, M.; and Lempitsky, V. 2016. Domain-adversarial training of neural networks. *The Journal of Machine Learning Research* 17(1):2096–2030.
- Ge, L.; Ren, Z.; Li, Y.; Xue, Z.; Wang, Y.; Cai, J.; and Yuan, J. 2019. 3d hand shape and pose estimation from a single rgb image.
- Gomezdonoso, F.; Ortsescolano, S.; and Cazorla, M. 2019. Large-scale multiview 3d hand pose dataset. *Image and Vision Computing* 81:25–33.
- Gulrajani, I.; Ahmed, F.; Arjovsky, M.; Dumoulin, V.; and Courville, A. C. 2017. Improved training of wasserstein gans. In Guyon, I.; Luxburg, U. V.; Bengio, S.; Wallach, H.; Fergus, R.; Vishwanathan, S.; and Garnett, R., eds., *Advances in Neural Information Processing Systems 30*. Curran Associates, Inc. 5767–5777.
- Iqbal, U.; Molchanov, P.; Breuel Juergen Gall, T.; and Kautz, J. 2018. Hand pose estimation via latent 2.5d heatmap regression. In *The European Conference on Computer Vision (ECCV)*.
- Li, H.; Jialin Pan, S.; Wang, S.; and Kot, A. C. 2018. Domain generalization with adversarial feature learning. In *The IEEE Conference on Computer Vision and Pattern Recognition (CVPR)*.
- Maaten, L. v. d., and Hinton, G. 2008. Visualizing data using t-sne. *Journal of machine learning research* 9(Nov):2579–2605.
- Mueller, F.; Mehta, D.; Sotnychenko, O.; Sridhar, S.; Casas, D.; and Theobalt, C. 2017. Real-time hand tracking under occlusion from an egocentric rgb-d sensor. In *Proceedings of International Conference on Computer Vision (ICCV)*, volume 10.
- Mueller, F.; Bernard, F.; Sotnychenko, O.; Mehta, D.; Sridhar, S.; Casas, D.; and Theobalt, C. 2018. Generated hands for real-time 3d hand tracking from monocular rgb. In *The IEEE Conference on Computer Vision and Pattern Recognition (CVPR)*.
- Newell, A.; Yang, K.; and Deng, J. 2016. Stacked hourglass networks for human pose estimation. In *European Conference on Computer Vision*, 483–499. Springer.
- Oreshkin, B.; López, P. R.; and Lacoste, A. 2018. Tadam: Task dependent adaptive metric for improved few-shot learning. In *Advances in Neural Information Processing Systems*, 721–731.
- Rad, M.; Oberweger, M.; and Lepetit, V. 2018a. Domain transfer for 3d pose estimation from color images without manual annotations. *asian conference on computer vision* 69–84.
- Rad, M.; Oberweger, M.; and Lepetit, V. 2018b. Feature mapping for learning fast and accurate 3d pose inference from synthetic images. In *The IEEE Conference on Computer Vision and Pattern Recognition (CVPR)*.
- Sankaranarayanan, S.; Balaji, Y.; Jain, A.; Nam Lim, S.; and Chellappa, R. 2018. Learning from synthetic data: Addressing domain shift for semantic segmentation. In *The IEEE Conference on Computer Vision and Pattern Recognition (CVPR)*.
- Shen, J.; Qu, Y.; Zhang, W.; and Yu, Y. 2018. Wasserstein distance guided representation learning for domain adaptation. *national conference on artificial intelligence* 4058–4065.
- Spurr, A.; Song, J.; Park, S.; and Hilliges, O. 2018. Cross-modal deep variational hand pose estimation. In *The IEEE Conference on Computer Vision and Pattern Recognition (CVPR)*, 89–98.
- Sun, X.; Shang, J.; Liang, S.; and Wei, Y. 2017. Compositional human pose regression. In *The IEEE International Conference on Computer Vision (ICCV)*.
- Tzeng, E.; Hoffman, J.; Saenko, K.; and Darrell, T. 2017. Adversarial discriminative domain adaptation. In *The IEEE Conference on Computer Vision and Pattern Recognition (CVPR)*.
- Villani, C., and dric. 2009. Optimal transport. *Grundlehren Der Mathematischen Wissenschaften* 338:xxii+973.
- Yang, W.; Ouyang, W.; Wang, X.; Ren, J.; Li, H.; and Wang, X. 2018. 3d human pose estimation in the wild by adversarial learning. In *The IEEE Conference on Computer Vision and Pattern Recognition (CVPR)*.
- Zhang, J.; Jiao, J.; Chen, M.; Qu, L.; Xu, X.; and Yang, Q. 2017. A hand pose tracking benchmark from stereo matching. In *2017 IEEE International Conference on Image Processing, ICIP 2017, Beijing, China, September 17-20, 2017*, 982–986.
- Zhou, X.; Huang, Q.; Sun, X.; Xue, X.; and Wei, Y. 2017. Towards 3d human pose estimation in the wild: A weakly-supervised approach. In *The IEEE International Conference on Computer Vision (ICCV)*.
- Zhu, J.-Y.; Park, T.; Isola, P.; and Efros, A. A. 2017. Unpaired image-to-image translation using cycle-consistent adversarial networks. In *The IEEE International Conference on Computer Vision (ICCV)*.
- Zimmermann, C., and Brox, T. 2017. Learning to estimate 3d hand pose from single rgb images. In *The IEEE International Conference on Computer Vision (ICCV)*.